The pitfalls of in vivo imaging techniques: evidence for cellular damage caused by synchrotron X-ray computed micro-tomography.

(Article begins on next page)

1 **The pitfalls of *in vivo* imaging techniques: evidence for cellular damage**

2 **caused by synchrotron X-ray computed micro-tomography**

3 F. Petruzzellis[1], C. Pagliarani[2,5], T. Savi[1,3], A. Losso[4], S. Cavalletto[5], G. Tromba[6], C. Dullin[6,7,8], A.

4 Ganthaler[4], A. Miotto[1], S. Mayr[4], M.A. Zwieniecki[9], A. Nardini[1]*, F. Secchi[5]

5

6 1. Dipartimento di Scienze della Vita, Università di Trieste, Via L. Giorgieri 10, 34127 Trieste, Italia

7 2. Institute for Sustainable Plant Protection, National Research Council, Strada delle Cacce 73, 10135

8 Torino, Italia

9 3. University of Natural Resources and Life Sciences, Division of Viticulture and Pomology,

10 Department of Crop Sciences, Konrad Lorenz Straße 24, A-3430 Tulln, Vienna, Austria

11 4. Department of Botany, University of Innsbruck, Sternwartestraße 15, 6020 Innsbruck, Austria

12 5. Dipartimento di Scienze Agrarie, Forestali e Alimentari, Università di Torino, Largo Paolo Braccini 2,

13 10095 Grugliasco (TO), Italia

14 6. Elettra-Sincrotrone Trieste, Area Science Park, 34149 Basovizza, Trieste, Italia

15 7. Institute for Diagnostic and Interventional Radiology, University Medical Center Göttingen, Robert-

16 Koch-Straße 40, 37075 Göttingen, Germany

17 8. Max-Plank-Institute for Experimental Medicine, Hermann-Rein-Straße 3, 37075 Göttingen,

18 Germany

19 9. Department of Plant Sciences, University of California Davis, One Shields Ave, Davis, CA 95616,

20 USA

21

22 * Corresponding author: nardini@units.it

23

24 **ABSTRACT**

25

26 • Synchrotron X-ray computed micro-tomography (microCT) has emerged as a promising non-
27 invasive technique for *in vivo* monitoring of xylem function, including embolism build-up under
28 drought and hydraulic recovery following re-irrigation. Yet, the possible harmful effects of ionizing
29 radiation on plant tissues have never been quantified.

30

31 • We specifically investigated the eventual damage suffered by stem living cells of three different
32 species exposed to repeated microCT scans. Stem samples exposed to one, two or three scans were
33 used to measure cell membrane and RNA integrity, and compared to controls never exposed to X-
34 rays.

35

36 • Samples exposed to microCT scans suffered serious alterations to cell membranes, as revealed by
37 marked increase in relative electrolyte leakage, and also underwent severe damage to RNA
38 integrity. The negative effects of X-rays were apparent in all species tested, but the magnitude of
39 damage and the minimum number of scans inducing negative effects were species-specific.

40

41 • Our data show that multiple microCT scans lead to disruption of fundamental cellular functions and
42 processes. Hence, microCT investigation of phenomena that depend on physiological activity of
43 living cells may produce erroneous results and lead to incorrect conclusions.

44

INTRODUCTION

In plants, long distance water transport relies on transmission of transpiration-induced negative pressure (= tension) via the xylem conduits connecting root tips to leaf cells (Jensen *et al.*, 2016). Such a fascinating mechanism has the important drawback to be metastable and vulnerable to liquid-to-vapor transition, leading to the blockage of water transport (Zimmermann, 1983). Most frequently, this happens when air is aspirated through inter-conduit pit membranes into water-filled conduits experiencing critical tensions (Shen *et al.*, 2015; Zwieniecki & Secchi, 2015). Increased frequency of drought and heat waves is accelerating plant mortality rates worldwide (Hember *et al.*, 2017), and hydraulic failure has emerged as the main cause (Anderegg *et al.*, 2011). A detailed knowledge of species-specific vulnerability to xylem embolism (Maherali *et al.*, 2004), and of the eventual capacity for hydraulic recovery (Mayr *et al.*, 2014; Secchi *et al.*, 2017; Klein *et al.*, 2018) is crucial to improve projections of forest and crop resistance/resilience under future climate scenarios.

Techniques used to measure plant hydraulic conductance upon drought and recovery are generally destructive (Cochard *et al.*, 2013). Stems, roots, petioles and even leaves are excised from plants during or after drought stress, and connected to hydraulic systems to measure flow rates across samples under known pressure differences (Sperry *et al.*, 1988). Alternatively, tissues can be infiltrated with dyes to distinguish functioning *versus* embolized or otherwise non-conducting conduits (Ewers & Fisher, 1989). Due to negative pressure in functional xylem conduits, samples' excision might cause air entry in the xylem, producing artefactual embolism (Wheeler *et al.*, 2013). The magnitude of this artefact may depend on xylem pressure at sampling time and on conduit length (Beikircher & Mayr, 2016). Although several studies found no striking evidence for artefacts associated with classical hydraulic techniques (Jacobsen & Pratt, 2012; Trifilò *et al.*, 2014; Fukuda *et al.*, 2015; Hacke *et al.*, 2015; Scoffoni & Sack, 2015; Venturas *et al.*, 2015; Ogasa *et al.*, 2016; Nardini *et al.*, 2017; Nolf *et al.*, 2017), it is conceivable that estimates of xylem vulnerability to embolism and restoration of xylem functionality (recovery) (Nardini *et al.*, 2018), are biased by destructive sampling protocols.

These controversies have contributed to move forward the field of plant hydraulics (Jansen *et al.*, 2015; Venturas *et al.*, 2017), and stimulated the use of non-destructive techniques for *in vivo* monitoring of xylem function, like magnetic resonance imaging (Zwieniecki *et al.*, 2013), X-ray computed micro-tomography (microCT; Brodersen *et al.*, 2010), and the optical method applied to leaf venation (Brodribb *et al.*, 2016). In particular, microCT has emerged as a very promising technology, due to relatively ease of use, high spatial and temporal resolution, good contrast between air-filled and water-filled spaces, and fast scan times (Dhondt *et al.*, 2010; Pajor *et al.*, 2013; Cochard et al., 2015). Due to its supposed non-invasive nature, microCT has been suggested to

80   represent a reference technique to determine xylem vulnerability to embolism (Cochard *et al.*, 2015),

81   and the eventual refilling of embolized conduits which supposedly relies on the activity of living

82   xylem parenchyma cells (Tyree *et al.*, 1999; Brodersen & McElrone, 2013; Secchi *et al.*, 2017; Nardini

83   *et al.*, 2018). While some studies demonstrated the occurrence of conduit refilling (Brodersen *et al.*,

84   2010; Brodersen *et al.*, 2018), others failed to detect hydraulic recovery following drought and re-

85   irrigation (Choat *et al.*, 2015; Knipfer *et al.*, 2015; Charrier *et al.*, 2016; Hochberg *et al.*, 2016).

86   These contrasting findings raise questions about possible factors affecting the reliability of

87   microCT observations (Pratt & Jacobsen, 2018). An obvious but often overlooked drawback of

88   microCT is the use of X-ray sources and the potential tissue damage caused by the ionizing radiation

89   (Han & Yu, 2009; Daly, 2012). Although this has been considered a minor issue because of short scan

90   times, some studies on animal organisms indicated irreversible cellular damage even by exposure to

91   very low X-ray doses (Rothkamm & Löbrich, 2003; Nguyen *et al.*, 2015). However, respective X-rays

92   effect on plant samples have never been investigated in details, although previous studies indicated

93   damage of plant tissues after microCT scans. As an example, Charrier *et al.* (2016) used vital staining

94   to assess the functional status of stem parenchyma cells after exposure to X-rays, showing that

95   several cells were damaged. Similarly, Savi *et al.* (2017) reported shrinkage and brownish scar

96   formation in sunflower stems exposed to X-rays. Hence, it is very important and urgent to test

97   eventual negative or otherwise undesired effects of X-rays on the observed samples, considering the

98   raising importance of microCT as a tool for studies on plant hydraulic functioning. Here, we discuss

99   the results from an experiment specifically designed to assess eventual damage to stem living cells

100   during repeated microCT scans.

101

102   **MATERIALS AND METHODS**

103

104   Plant material

105   Experiments were performed on three species: *Helianthus annuus*, *Coffea arabica* cv. Pacamara, and

106   *Populus tremula x alba*. *H. annuus* plants were six-week old, with a height of about 20 cm and a stem

107   diameter of 2-3 mm at root collar. *C. arabica* plants were part of a collection of coffee cultivars

108   hosted by Univ. Trieste. Experimental plants were three-year-old, with a height of 20-30 cm, and a

109   stem diameter of 3-4 mm. Plants of *P. tremula x alba* were three-months-old, approximately 50 cm

110   tall with a stem diameter of 3-4 mm.

111   All plants were maintained in a greenhouse at Univ. Trieste for 4 weeks before experiments

112   (end of September 2017), and regularly watered. Air temperature and relative humidity averaged

113   16.5 °C and 60%, respectively. Mean daily photosynthetic photon flux density (PPFD) was 150 µmol

114   m^{-2} s^{-1} (maximum 400 µmol m^{-2} s^{-1}).

115

116 <u>Experimental setup</u>

117   Experiments were performed at the SYRMEP beamline, Elettra Sincrotrone Trieste

118 (www.elettra.trieste.it). Two silicon filters (0.5 mm each) were used to obtain an average X-ray

119 source energy of 25 keV, resulting in an entrance dose rate in water of 47 mGy s^{-1}. X-ray window was

120 4 mm in height with horizontal opening up to 120 mm. Initial experiments were performed on intact

121 plants of *H. annuus* and *P. tremula x alba* (n = 3) to test for eventual over-heating of stems as a

122 possible factor inducing damage during scans. A type T thermocouple connected to a datalogger

123 (1000 Series Squirrel, Eltek) was inserted in the stem at half height. The plant was placed on the

124 sample holder and the stem was aligned with the beam. The beam was turned off to allow

125 temperature equilibration for 5 min. Then, the stem was irradiated for 10 min at a position located 8

126 mm above the thermocouple insertion point, while temperature was continuously recorded. After a

127 5 min interval without beam, the stage was moved upward and the stem was irradiated 3 mm above

128 the thermocouple, for another 10 min. The procedure was repeated by directly irradiating the

129 thermocouple insertion point.

130   The cellular damage caused by microCT scans was assessed by measuring cell membrane

131 integrity estimated by relative electrolyte leakage (REL), and level of RNA degradation on irradiated

132 stem tissues. Stem segments with a length of 1 cm (n = 5) were obtained from the mid portion of

133 stems of well hydrated plants, and immediately wrapped in Parafilm® in groups of 5 (sampled from 5

134 different plants). This allowed to prevent desiccation during storage (see below) and to irradiate

135 more samples during each scan. For each species, 14 sample sets (each with 5 stem pieces) were

136 prepared (total of 70 stem samples per species).

137   Samples were subjected to microCT scans while horizontally oriented to assure that all cells

138 were exposed to X-rays during the 360° rotation (the position was checked via real-time

139 visualization). The exposure time was set at 100 ms, at an angular step of 2° s^{-1} resulting in 3 min

140 scan. Samples were then used to measure REL (7 sets) and RNA quality (7 sets), according to

141 experimental design presented in Fig. 1. Exposed samples were tested after one, two, or three

142 consecutive scans at 90 minutes intervals (E1, E2, and E3). Controls (C0, C1, C2, C3) were never

143 exposed to irradiation. Time of exposure and beam energy level was similar to previously reported

144 experiments (e.g. Charrier *et al.*, 2016), although not all experiments are provided with energy level

145 parameter.

146   The integrity of cell membranes was estimated via REL measurements. C or E samples were

147 placed in 1.5 ml vials (1 segment per vial) with 1 ml of deionized water. In the case of *C. arabica* and

148 *P. tremula x alba*, segments were split longitudinally immediately before immersion to favor contact

149 between stem cells and the solution, as preliminary experiments showed that the bark delayed

150   solute diffusion. The tubes were shaken for 30 min at laboratory temperature. The initial electrical

151   conductivity (C_i) of the solution was measured (Twin Cond B-173, Horiba, Kyoto, Japan) using a 10 µl

152   aliquot. Samples were then subjected to 3 freezing-thawing cycles (1 min in liquid nitrogen followed

153   by 30 min at laboratory temperature), shaken for 5 min, and the final electrical conductivity was

154   measured (C_f) on another 10 µl aliquot. REL was finally calculated as (C_i/C_f) × 100 (Savi *et al.*, 2016).

155   For RNA analysis, frozen stems for each species and treatment were pooled and ground in

156   sterile mortars using liquid nitrogen followed by tissue lysing (TissueLyser II, Qiagen). Total RNA was

157   extracted following Chang *et al.* (1993), and RNA quantity and quality were determined

158   spectrophotometrically by NanoDrop (Thermo Fisher Scientific). RNA integrity (expressed as RNA

159   integrity number, RIN; Schroeder *et al.*, 2006) was finally inspected using the RNA 6000 Nano kit and

160   the Agilent 2100 Bioanalyzer (Agilent Technologies), according to manufacturer's instructions. The

161   RNA Integrity Number (RIN) is a standard reference for RNA quality assessment, specifically

162   introduced in routine RNA quality control processes to avoid subjective interpretation of results. The

163   RIN values resulting at the end of each Bionalyzer run provide a classification of total RNA quality,

164   based on a numbering system ranging from 1 (poor quality and high level of degradation) to 10 (high

165   quality and high integrity levels). As RNA degradation proceeds, there is a decrease in the 18S to 28S

166   ribosomal RNA band ratio and an increase in the background noise between the 18 and 28 ribosomal

167   peaks (Bioanalyzer user guide). In Fig. 4, the 18S ribosomal band is visible at 40-42 s time, while the

168   28S ribosomal band at 46 s time.

169

170   <u>Statistical analysis</u>

171   One-way parametric ANOVA analysis was run separately for each species to test differences between

172   REL values measured in C and E samples through "aov" function in "stats" package for R software (R

173   Development Core Team 2017). Data were log transformed to meet assumptions of normality and

174   homoscedasticity of variance. Post-hoc Tukey's Honestly Significant Differences comparisons were

175   run through "TukeyHSD" function in "stats" package for R.

176

177   **RESULTS**

178

179   Exposing stems of *H. annuus* or *P. tremula x alba* to X-rays did not did not result in biologically

180   significant changes in tissue temperature (Fig. 2). Stem temperature oscillated between 25 and 26 °C

181   with no beam, and no change was detected at a distance of 3 or 8 mm from the irradiated point even

182   under prolonged exposure (10 min). Temperature in stem section directly exposed to radiation rose

183   by about 1°C in both tested species.

184   Cell membrane integrity, quantified via REL measurements, was affected by X-ray exposure in
185   analyzed species (Fig. 3). In all plants, REL of C0 samples was about 25%, and this value did not
186   change significantly as a function of time from excision in C1, C2 and C3 samples (Fig. 3). In the case
187   of *H. annuus*, the first scan did not induce changes in REL, however these became apparent in E2 and
188   E3, when REL peaked to 70%, with some samples reaching values as high as 90%. In *P. tremula x alba*,
189   REL increased to 35% in E2, and remained similar in E3. In *C. arabica* an increase of REL to 45% (albeit
190   not significant due to large data variability) was already observed in E1 samples, reaching values >
191   50% in E3.

192   Total RNA quality was estimated by the RNA Integrity Number (RIN), as this is a reliable proxy
193   to compare the integrity of RNA in different samples. Analyses based on this metric confirmed the
194   results obtained by REL measurements, showing similar variability and resistance of species to
195   radiation (Fig. 4). In the case of *H. annuus*, the first scan did not affect RNA quality (E1, 7.5). However,
196   RNA degradation increased after the second exposure, and the RNA after the third exposure (E3) was
197   almost fully degraded (Fig. 4). In this species, the controls (C0-C3) showed no degradation of RNA
198   quality. There was no effect of time or X-ray exposures on RNA quality of samples collected from P*.*
199   *tremula x alba* stems, although E3 samples had slightly lower RNA quality (RIN 6.2; Fig. 4). After one
200   scan, RNA extracted from *C. arabica* was partially degraded (E1; RIN 4.1), in comparison to controls
201   (C1, RIN 7). However, both X-ray exposures and time from excision influenced the RNA quality in this
202   species (see C2-3 and E2-3; Fig. 4) confirming that *C. arabica* was sensitive to both manipulation and
203   X-rays.

204
205   **DISCUSSION**
206
207   X-ray microCT is emerging as an important new tool for the visualization and quantification of xylem
208   embolism (Cochard *et al.*, 2015). Based on its supposed non-invasive nature, microCT has also been
209   used to visualize eventual post-drought embolism recovery. In both cases, plants are generally
210   exposed to successive microCT scans to check embolism build-up during plant dehydration (Choat *et*
211   *al.*, 2016), or its reversal following re-watering (Charrier *et al.*, 2016).

212   Xylem conduits are frequently considered as inert pipelines, but long-distance water
213   transport relies on the activity of phloem and parenchyma, e.g. for the regulation of xylem sap ionic
214   content (Zwieniecki *et al.*, 2001; Nardini *et al.*, 2011), modulation of xylem sap surface tension (Losso
215   *et al.*, 2017), release of sugars and water during the refilling of embolized conduits (Secchi *et al.*,
216   2017), and production of conduit-filling exudates as a response to wounds (Jacobsen *et al.*, 2018).
217   Hence, any eventual damage to living cells can be suspected to alter xylem function, thus casting
218   doubts on the reliability of techniques inducing harmful effects on phloem or parenchyma. Our data

219 clearly show that microCT scans produce severe cellular damage, and call for renewed caution in the

220 interpretation of findings based on this technique (Pratt & Jacobsen, 2018). The X-ray energy level

221 and scan times in our experiment were similar to or even lower than those used in several recent

222 studies (e.g. Charrier *et al.*, 2016; Choat *et al.*, 2016; Knipfer *et al.*, 2017). Yet, the X-ray dose was

223 high enough to induce damage to both cell membranes and RNA.

224 Samples exposed to microCT scans showed significant increases in REL, indicating serious

225 alterations to cell membranes. This is not surprising, as several studies have shown that X-rays

226 produce irreversible damage to membrane lipid bilayers due to phase transformation and lamellar

227 stacking (Köteles, 1982; Cheng & Caffrey, 1996; Cherezov *et al.*, 2002), with consequent effects on

228 membrane permeability (Cao *et al.*, 2015). Cherezov *et al.* (2002) reported that membrane damage is

229 not associated to temperature effects during sample irradiation at synchrotron light sources, as also

230 confirmed by the lack of over-heating recorded in our samples, but it rather depends on generation

231 of free radicals. Most importantly, Cherezov *et al.* (2002) evidenced that the damage was

232 independent on the source energy in a 9-17 keV range, suggesting that the risk of membrane damage

233 is intrinsic to the technique and cannot be reduced by modifying X-ray energy level without losing

234 image quality and resolution.

235 In addition to disruption of cell membranes, our data indicate that microCT scans negatively

236 affect RNA quality. This is also not unexpected, as ionizing radiation is known to induce significant

237 alterations on nucleic acids, often resulting in DNA double strand breaks (Rothkamm & Löbrich, 2003;

238 Han & Yu, 2009) and ROS-mediated DNA/RNA disruption (van Huystee *et al.*, 1968; Tominaga *et al.*,

239 2004), finally leading to severe RNA and/or protein damage (Daly, 2012). Our data from plants are in

240 line with findings obtained on animal cell models, and suggest that, as a consequence of RNA

241 damage, protein synthesis can be impaired in stem parenchyma cells after microCT scans.

242 Both membrane damage and RNA degradation were observed in three studied species, but

243 the susceptibility to X-rays damage was species-specific. *C. arabica* was damaged by a single scan,

244 while two-three scans were necessary to produce significant effects in other two species. It is

245 possible that not all microCT experiments performed on different species and reported in the

246 literature are affected to the same extent by harmful radiation effects, potentially explaining the

247 observed range of hydraulic recovery in different species (Choat *et al.*, 2015; Knipfer *et al.*, 2015;

248 Charrier *et al.*, 2016; Brodersen *et al.*, 2018). Our findings call for a careful reassessment of previous

249 conclusions, based on dedicated experiments to evaluate the susceptibility of individual species to

250 the specific experimental conditions adopted.

251 Our data show that multiple microCT scans lead to disruption of fundamental cellular

252 functions and processes. Hence, microCT investigation of phenomena that depend on physiological

253 activity of living cells may produce erroneous results and lead to incorrect conclusions. This probably

applies to conduit refilling, which has been suggested to occur via secretion of sugars into embolized conduits by phloem and vessel-associated parenchyma cells to generate the osmotic forces necessary to counterbalance eventual residual tension in still functioning elements (Secchi & Zwieniecki, 2012). Such a mechanism requires the activation of genes encoding key proteins involved in carbohydrate metabolism pathways and membrane transport of inorganic ions, sugar molecules, and water (Secchi *et al.*, 2011; Perrone *et al.*, 2012; Chitarra *et al.*, 2014; Secchi *et al.*, 2016). Thus, failure in detecting embolism reversal in microCT experiments, when involving repeated scans of the same plant subjected to drought stress and then re-irrigated (Choat *et al.*, 2015; Knipfer *et al.*, 2015; Charrier *et al.*, 2016; Knipfer *et al.*, 2017), might arise from X-ray induced damage to living cells. We strongly suggest that such evidence should be re-evaluated in the light of our findings, and also recommend that xylem vulnerability or recovery curves generated by microCT should be based on sets of different plants, so that a single plant at any given water status or physiological stage is scanned and observed only once if the species is susceptible to applied radiation levels. Although this approach might raise doubts on the advantages of microCT as an alternative or complementary technique with respect to classical hydraulic measurements, it would still yield important information or confirmation on the functional status of conduits with no risk of bias due to cutting procedures.

MicroCT observations are increasingly used to observe xylem embolism build-up during plant dehydration. It is assumed that embolism spreads by aspiration of air through the pores of inter-conduit remnants of primary cell walls and middle lamella (pit membranes). Thus, the validity of observations of embolism spread is seemingly not challenged by our findings, unless X-rays disrupt and alter the structure and porosity of pit membranes, leading to erroneous estimates of embolism vulnerability. Also, damage to living cells might result in wound responses leading to rapid filling of xylem conduits with gels (Crews *et al.*, 2003; Soukup & Votrubová, 2005; Marañón-Jiménez *et al.*, 2017; Che-Husin *et al.*, 2018; Jacobsen *et al.*, 2018). Such an effect would cause conduits to appear filled with a liquid phase even though non-conducting (Pratt & Jacobsen, 2018), leading to overestimate plant resistance to xylem embolism. The occurrence and relevance of these effects should be evaluated by future studies.

AUTHOR CONTRIBUTIONS

A.N., F.S., M.Z., and S.M. planned and designed the research. All Authors contributed to perform experiments and analyze data. F.P., A.N. and F.S. wrote the manuscript, with contribution and revision by all Authors.

REFERENCES

Anderegg WRL, Berry JA, Smith DD, Sperry JS, Anderegg LDL, Field CB. 2011. The roles of hydraulic and carbon stress in a widespread climate-induced forest die-off. *Proceedings of the National Academy of Sciences USA* **109:** 233-237.

Beikircher B, Mayr S. 2016. Avoidance of harvesting and sampling artefacts in hydraulic analyses: a protocol tested on *Malus domestica*. *Tree Physiology* **36:** 797-803.

Brodersen CR, Knipfer T, McElrone AJ. 2018. In vivo visualization of the final stages of xylem vessel refilling in grapevine (*Vitis vinifera*) stems. *New Phytologist* **217:** 117-126.

Brodersen CR, McElrone AJ. 2013. Maintenance of xylem network transport capacity: a review of embolism repair in vascular plants. *Frontiers in Plant Science* **4:** 108.

Brodersen CR, McElrone AJ, Choat B, Matthews MA, Shackel KA. 2010. The dynamics of embolism repair in xylem: in vivo visualizations using high-resolution computed tomography. *Plant Physiology* **154:** 1088-1095.

Brodribb TJ, Skelton RP, McAdam SAM, Bienaimé D, Lucani CJ, Marmottant P. 2016. Visual quantification of embolism reveals leaf vulnerability to hydraulic failure. *New Phytologist* **209:** 1403-1409.

Cao G, Zhang M, Miao J, Li W, Wang J, Lu D, Xia J. 2015. Effects of X-ray and carbon ion beam irradiation on membrane permeability and integrity in *Saccharomyces cerevisiae* cells. *Journal of Radiation Research* **56:** 294-304.

Chang S, Puryear J, Cairney J. 1993. A simple and efficient method for isolating RNA from pine tree. *Plant Molecular Biology Report* **11:** 113-116.

Charrier G, Torres-Ruiz JM, Badel E, Burlett R, Choat B, Cochard H, Delmas CEL, Domec JC, Jansen S, King A, Lenoir N, Martin-StPaul N, Gambetta GA, Delzon S. 2016. Evidence for hydraulic vulnerability segmentation and lack of xylem refilling under tension. *Plant Physiology* **172:** 1657-1668.

Che-Husin NM, Joyce DC, Irving DE. 2018. Gel xylem occlusions decrease hydraulic conductance of cut *Acacia holosericea* foliage stems. *Postharvest Biology and Technology* **135:** 27-37.

Cheng A, Caffrey M. 1996. Free radical mediated X-ray damage of model membranes. *Biophysical Journal* **70:** 2212-2222.

Cherezov V, Riedl KM, Caffrey M. 2002. Too hot to handle? Synchrotron X-ray damage of lipid membranes and mesophases. *Journal of Synchrotron Radiation* **9:** 333-341.

Chitarra W, Balestrini R, Vitali M, Pagliarani C, Perrone I, Schubert A, Lovisolo C. 2014. Gene expression in vessel–associated cells upon xylem embolism repair in *Vitis vinifera* L. petioles. *Planta* **239:** 887-899.

Choat B, Brodersen CR, McElrone AJ. 2015. Synchrotron X-ray microtomography of xylem embolism in *Sequoia sempervirens* saplings during cycles of drought and recovery. *New Phytologist* **205:** 1095-1105.

Choat B, Badel E, Burlett R, Delzon S, Cochard H, Jansen S. 2016. Noninvasive measurement of vulnerability to drought-induced embolism by X-ray microtomography. *Plant Physiology* **170:** 273-282.

Cochard H, Badel E, Herbette S, Delzon S, Choat B, Jansen S. 2013. Methods for measuring plant vulnerability to cavitation: a critical review. *Journal of Experimental Botany* **64:** 4779-4791.

Cochard H, Delzon S, Badel E. 2015. X-ray microtomography (microCT): a reference technology for high-resolution quantification of xylem embolism in trees. *Plant, Cell & Environment* **38:** 201-206.

338 **Crews LJ, McCully ME, Canny MJ. 2003.** Mucilage production by wounded xylem tissue of maize
339   roots - time course and stimulus. *Functional Plant Biology* **30:** 755-766.
340 **Daly MJ. 2012.** Death by protein damage in irradiated cells. *DNA Repair* **11:** 12-21.
341 **Dhondt S, Vanhaeren H, Van Loo D, Cnudde V, Inzé D. 2010.** Plant structure visualization by high-
342   resolution X-ray computed tomography. *Trends in Plant Science* **15:** 419-422.
343 **Ewers FW, Fisher JB. 1989.** Techniques for measuring vessel lengths and diameters in stems of
344   woody plants. *American Journal of Botany* **76:** 645-656.
345 **Fukuda K, Kawaguchi D, Aihara T, Ogasa MY, Miki NH, Haishi T, Umebayashi T. 2015.** Vulnerability
346   to cavitation differs between current-year and older xylem: non-destructive observation with a
347   compact magnetic resonance imaging system of two deciduous diffuse-porous species. *Plant, Cell &*
348   *Environment* **38:** 2508-2518.
349 **Hacke UG, Venturas MD, MacKinnon ED, Jacobsen AL, Sperry JS, Pratt RB. 2015.** The standard
350   centrifuge method accurately measures vulnerability curves of long-vesselled olive stems. *New*
351   *Phytologist* **205:** 116-127.
352 **Han W, Yu KN. 2009.** Response of cells to ionizing radiation. In: Tjong SC, ed. *Advances in Biomedical*
353   *Sciences and Engineering*. Bentham Science Publisher Ltd, 204-262.
354 **Hember RA, Kurz WA, Coops NC. 2017.** Relationships between individual-tree mortality and water-
355   balance variables indicate positive trends in water stress-induced tree mortality across North
356   America. *Global Change Biology* **23:** 1691-1710.
357 **Hochberg U, Herrera JC, Cochard H, Badel E. 2016.** Short-time xylem relaxation results in reliable
358   quantification of embolism in grapevine petioles and sheds new light on their hydraulic strategy.
359   *Tree Physiology* **36:** 748-755.
360 **Jacobsen AL, Pratt RB. 2012.** No evidence for an open vessel effect in centrifuge-based vulnerability
361   curves of a long-vesselled liana (*Vitis vinifera*). *New Phytologist* **194:** 982-990.
362 **Jacobsen AL, Valdovinos-Ayala J, Pratt RB. 2018.** Functional lifespans of xylem vessels:
363   Development, hydraulic function, and post-function of vessels in several species of woody plants.
364   *American Journal of Botany* **105:** 142-150.
365 **Jansen S, Schuldt B, Choat B. 2015.** Current controversies and challenges in applying plant hydraulic
366   techniques. *New Phytologist* **205:** 961-964.
367 **Jensen KH, Berg-Sørensen K, Bruus H, Holbrook NM, Liesche J, Schulz A, Zwieniecki MA, Bohr T.**
368   **2016.** Sap flow and sugar transport in plants. *Reviews of Modern Physics* **88:** 035007.
369 **Klein T, Zeppel MJB, Anderegg WRL, Bloemen J, De Kauwe MG, Hudson P, Ruehr NK, Powell TL, von**
370   **Arx G, Nardini A. 2018.** Xylem embolism refilling and resilience against drought-induced mortality
371   in woody plants: processes and trade-offs. *Ecological Research* doi:10.1007/s11284-018-1588-y
372 **Knipfer T, Brodersen CR, Zedan A, Kluepfel DA, McElrone AJ. 2015.** Patterns of drought-induced
373   embolism formation and spread in living walnut saplings visualized using X-ray microtomography.
374   *Tree Physiology* **35:** 744-755.
375 **Knipfer T, Cuneo IF, Earles JM, Reyes C, Brodersen CR, McElrone AJ. 2017.** Storage compartments
376   for capillary water rarely refill in an intact woody plant. *Plant Physiology* **175:** 1649-1660.
377 **Köteles GJ. 1982.** Radiation effects on cell membranes. *Radiation and Environmental Biophysics* **21:**
378   1-18.
379 **Losso A, Beikircher B, Dämon B, Kikuta S, Schmid P, Mayr S. 2017.** Xylem sap surface tension may be
380   crucial for hydraulic safety. *Plant Physiology* **175:** 1135-1143.
381 **Maherali H, Pockman WT, Jackson RB. 2004.** Adaptive variation in the vulnerability of woody plants
382   to xylem cavitation. *Ecology* **85:** 2184-2199.
383 **Marañón-Jiménez S, Van den Bulcke J, Piayda A, Van Acker J, Cuntz M, Rebmann C, Steppe K. 2017.**
384   X-ray computed microtomography characterizes the wound effect that causes sap flow
385   underestimation by thermal dissipation sensors. *Tree Physiology* **38:** 288-302.
386 **Mayr S, Schmid P, Laur J, Rosner S, Charra-Vaskou K, Dämon B, Hacke UG. 2014.** Uptake of water
387   via branches helps timberline conifers refill embolized xylem in late winter. *Plant Physiology* **164:**
388   1731-1740.

Nardini A, Salleo S, Jansen S. 2011. More than just a vulnerable pipeline: xylem physiology in the light of ion-mediated regulation of plant water transport. *Journal of Experimental Botany* **62:** 4701-4718.

Nardini A, Savi T, Losso A, Petit G, Pacilè S, Tromba G, Mayr S, Trifilò P, Lo Gullo MA, Salleo S. 2017. X-ray microtomography observations of xylem embolism in stems of *Laurus nobilis* are consistent with hydraulic measurements of percentage loss of conductance. *New Phytologist* **213:** 1068-1075.

Nardini A, Savi T, Trifilò P, Lo Gullo MA. 2018. Drought stress and the recovery from xylem embolism in woody plants. *Progress in Botany* **79:** 197-231.

Nguyen PK, Lee WH, Li YF, Hong WX, Hu S, Chan C, Liang G, Nguyen I, Ong SG, Churko J, Wang J, Altman RB, Fleischmann D, Wu JC. 2015. Assessment of the radiation effects of cardiac CT angiography using protein and genetic biomarkers. *JACC: Cardiovascular Imaging* **8:** 873-884.

Nolf M, Lopez R, Peters JMR, Flavel RJ, Koloadin LS, Young IM, Choat B. 2017. Visualization of xylem embolism by X-ray microtomography: a direct test against hydraulic measurements. *New Phytologist* **214:** 890-898.

Ogasa MY, Utsumi Y, Miki NH, Yazaki K, Fukuda K. 2016. Cutting stems before relaxing xylem tension induces artefacts in *Vitis coignetiae*, as evidenced by magnetic resonance imaging. *Plant, Cell & Environment* **39:** 329-337.

Pajor R, Fleming A, Osborne CP, Rolfe SA, Sturrock CJ, Mooney SJ. 2013. Seeing space: visualization and quantification of plant leaf structure using X-ray micro-computed tomography. *Journal of Experimental Botany* **64:** 385-390.

Perrone I, Pagliarani C, Lovisolo C, Chitarra W, Roman F, Schubert A. 2012. Recovery from water stress affects grape leaf petiole transcriptome. *Planta* **235:** 1383-1396.

Pratt RB, Jacobsen AL. 2018. Identifying which conduits are moving water in woody plants: a new HRCT-based method. *Tree Physiology* doi:10.1093/treephys/tpy034

Rothkamm K, Löbrich M. 2003. Evidence for a lack of DNA double-strand break repair in human cells exposed to very low X-ray doses. *Proceedings of the National Academy of Sciences USA* **100:** 5057-5062.

Savi T, Dal Borgo A, Love VL, Andri S, Tretiach M, Nardini A. 2016. Drought versus heat: what's the major constraint on Mediterranean green roof plants? *Science of the Total Environment* **566:** 753-760.

Savi T, Miotto A, Petruzzellis F, Losso A, Pacilè S, Tromba G, Mayr S, Nardini A. 2017. Drought-induced embolism in stems of sunflower: a comparison of in vivo micro-CT observations and destructive hydraulic measurements. *Plant Physiology & Biochemistry* **120:** 24-29.

Schroeder A, Mueller O, Stocker S, Salowsky R, Leiber M, Gassmann M, Lightfoot S, Menzel W, Granzow M, Ragg T. 2006. The RIN: an RNA integrity number for assigning integrity values to RNA measurements. *BMC Molecular Biology* **7:** 3.

Scoffoni C, Sack L. 2015. Are leaves 'freewheelin'? Testing for a Wheeler-type effect in leaf xylem hydraulic decline. *Plant, Cell & Environment* **38:** 534-543.

Secchi F, Gilbert ME, Zwieniecki MA. 2011. Transcriptome response to embolism formation in stems of *Populus trichocarpa* provides insight into signaling and the biology of refilling. *Plant Physiology* **157:** 1419-1429.

Secchi F, Pagliarani C, Zwieniecki MA. 2017. The functional role of xylem parenchyma cells and aquaporins during recovery from severe water stress. *Plant, Cell & Environment* **40:** 858-871.

Secchi F, Zwieniecki MA. 2012. Analysis of xylem sap from functional (nonembolized) and nonfunctional (embolized) vessels of *Populus nigra*: chemistry of refilling. *Plant Physiology* **160:** 955-964.

Secchi F, Zwieniecki MA. 2016. Accumulation of sugars in the xylem apoplast observed under water stress conditions is controlled by xylem pH. *Plant Cell & Environment* **39:** 2350-2360.

Shen F, Cheng Y, Zhang L, Gao R, Shao X. 2015. Experimental study of the types of cavitation by air seeding using light microscopy. *Tree Physiology* **35:** 1325-1332.

Soukup AS, Votrubová O. 2005. Wound-induced vascular occlusions in tissues of the reed *Phragmites australis*: their development and chemical nature. *New Phytologist* **167:** 415-424.

441 **Sperry JS, Donnelly JR, Tyree MT. 1988.** A method for measuring hydraulic conductivity and
442   embolism in xylem. *Plant, Cell & Environment* **11:** 35-40.
443 **Tominaga H, Kodama S, Matsuda N, Suzuki K, Watanabe M. 2004.** Involvement of reactive oxygen
444   species (ROS) in the induction of genetic instability by radiation. *Journal of Radiation Research* **45:**
445   181-188.
446 **Trifilò P, Raimondo F, Lo Gullo MA, Barbera PM, Salleo S, Nardini A. 2014.** Relax and refill: xylem
447   rehydration prior to hydraulic measurements favours embolism repair in stems and generate
448   artificially low PLC values. *Plant, Cell & Environment* **37:** 2491-2499.
449 **Tyree MT, Salleo S, Nardini A, Lo Gullo MA, Mosca R. 1999.** Refilling of embolized vessels in young
450   stems of Laurel. Do we need a new paradigm? *Plant Physiology* **120:** 11-21.
451 **Van Huystee RB, Jachymczyk W, Tester CF, Cherry JH. 1968.** X-irradiation effects on protein
452   synthesis and synthesis of messenger ribonucleic acid from peanut cotyledons. *The Journal of*
453   *Biological Chemistry* **243:** 2315-2320.
454 **Venturas MD, MacKinnon ED, Jacobsen AL, Pratt RB. 2015.** Excising stem samples underwater at
455   native tension does not induce xylem cavitation. *Plant, Cell & Environment* **38:** 1060-1068.
456 **Venturas MD, Sperry JS, Hacke UG. 2017.** Plant xylem hydraulics: what we understand, current
457   research, and future challenges. *Journal of Integrative Plant Biology* **59:** 356-389.
458 **Wheeler JK, Huggett BA, Tofte AN, Rockwell FE, Holbrook NM. 2013.** Cutting xylem under tension or
459   supersaturated with gas can generate PLC and the appearance of rapid recovery from embolism.
460   *Plant, Cell & Environment* **36:** 1938-1949.
461 **Zimmermann MH. 1983.** Xylem structure and the ascent of sap. Springer Verlag, Berlin.
462 **Zwieniecki MA, Melcher PJ, Ahrens ET. 2013.** Analysis of spatial and temporal dynamics of xylem
463   refilling in *Acer rubrum* L. using magnetic resonance imaging. *Frontiers in Plant Science* **4:** 265.
464 **Zwieniecki MA, Melcher PJ, Holbrook NM. 2001.** Hydrogel control of xylem hydraulic resistance in
465   plants. *Science* **291:** 1059-1062.
466 **Zwieniecki MA, Secchi F. 2015.** Threats to xylem hydraulic function of trees under 'new climate
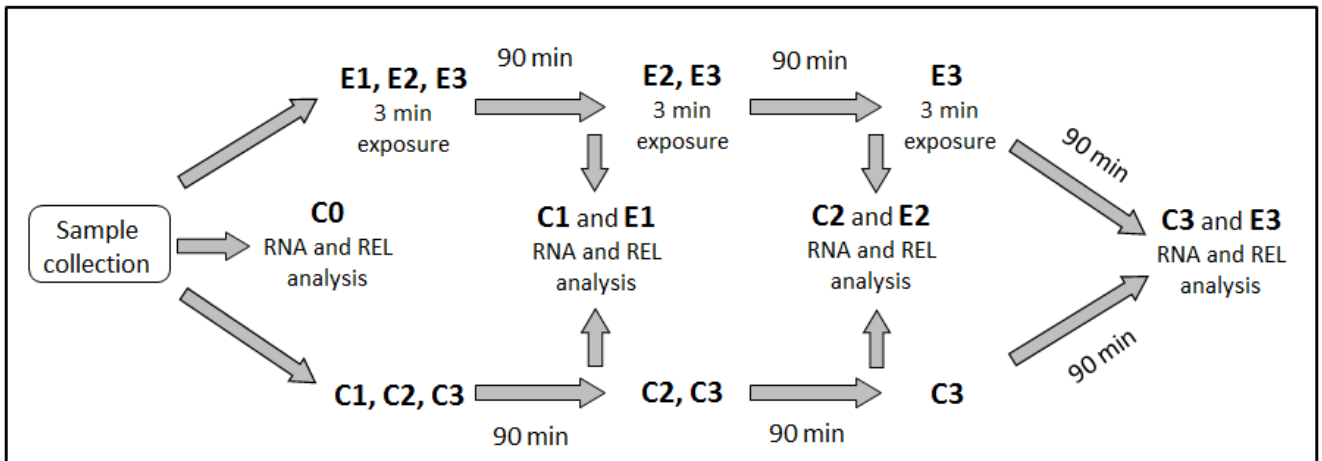467   normal' conditions. *Plant, Cell & Environment* **38:** 1713-1724.

Fig. 1: Experiment time line. C0: control samples i) immediately used for REL measurements or ii) frozen in liquid nitrogen and kept at -80 °C until RNA analysis. C1: samples excised from stems and stored at laboratory temperature until segments from group E1 were ready, then processed for REL or RNA analyses (see above). Samples C1, C2 and C3 were prepared to check eventual time-related trends in cellular damage not associated to X-rays exposure. E1: samples exposed to a single 3 min microCT scan (see below), maintained for 90 min at laboratory temperature to allow eventual damage build-up, then processed for REL or RNA analyses. C2: samples excised from stems and stored at laboratory temperature until samples from group E2 were ready, then processed for REL or RNA measurements. E2: samples exposed to two successive microCT scans (90 min between each exposure and afte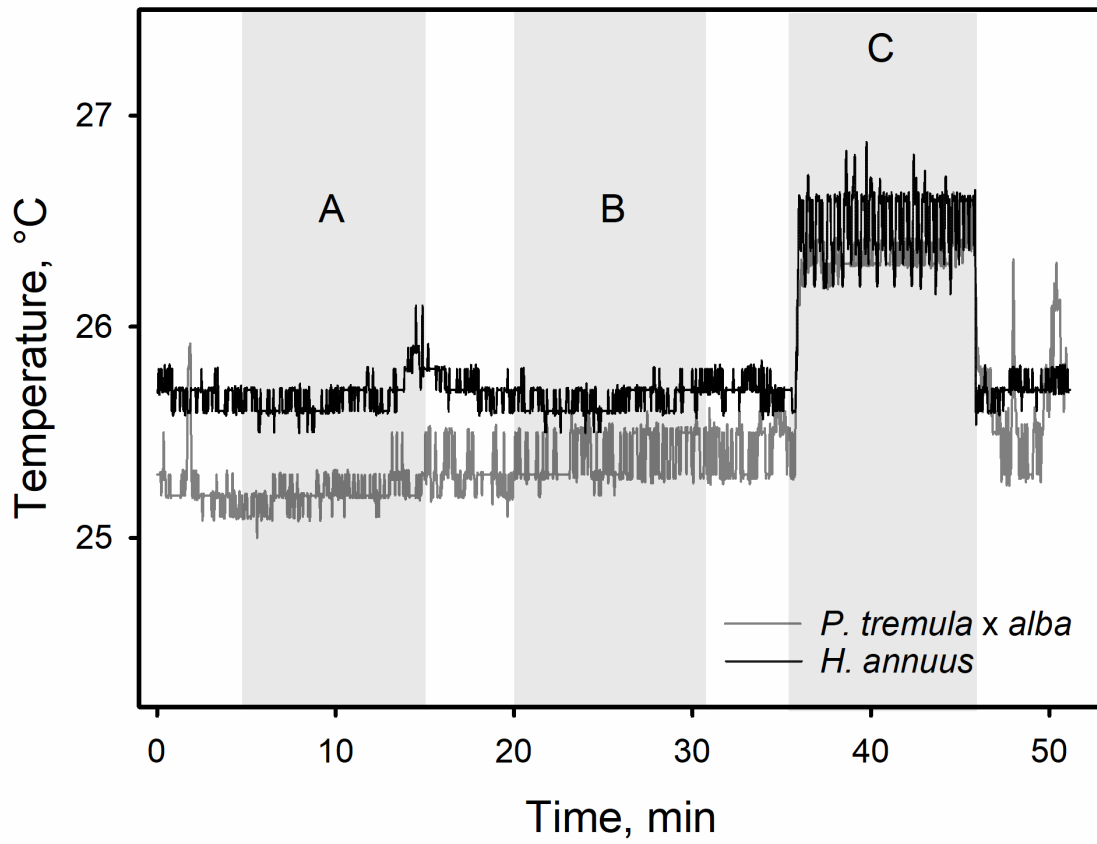r the last one), then processed for REL or RNA measurements. C3: samples excised from stems and stored at laboratory temperature until samples from group E3 were ready, then processed for REL or RNA measurements. E3: samples exposed to three successive microCT scans (90 min between each exposure and after the last one), then processed for REL or RNA measurements.

Fig. 2: Temperature changes over time in irradiated stems of *P. tremula* x *alba* (grey line) and *H. annuus* (black line) at 8 mm (A), 3 mm (B) and at the same position (C) of irradiation point.
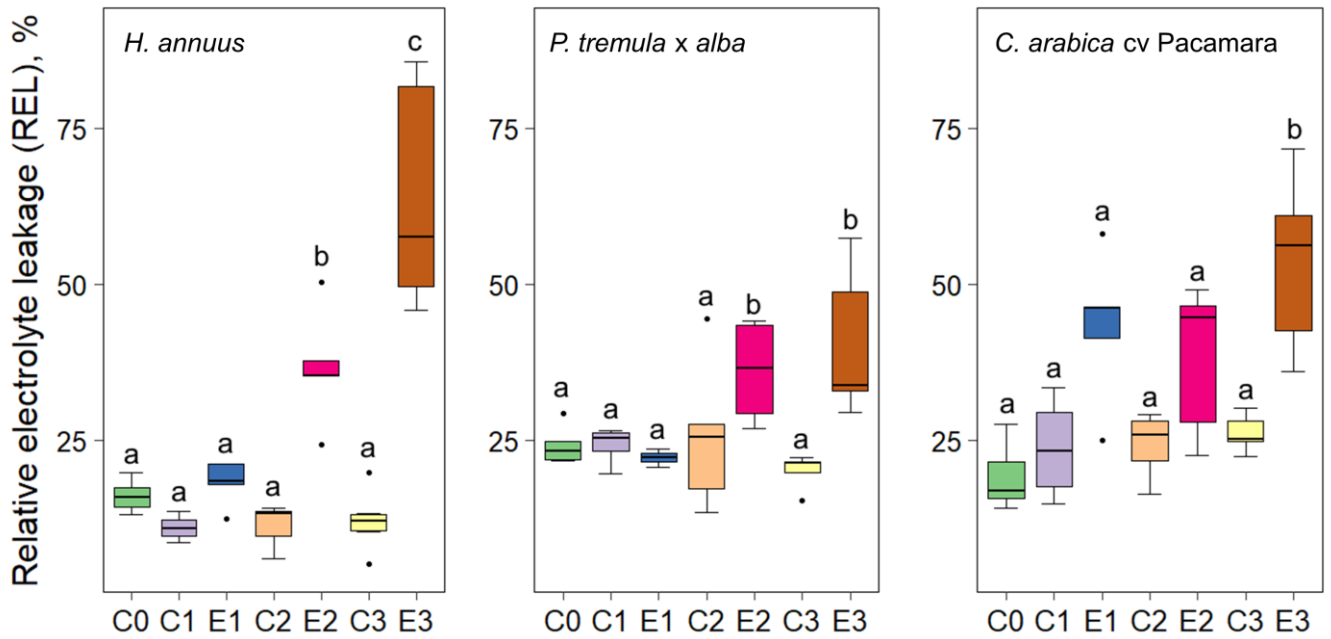
Fig. 3: Median values, 25th and 75th percentiles of relative electrolyte leakage (REL) in control and exposed sample groups in *H. annuus*, *P. tremula x alba* and in *C. arabica* cv. Pacamara. Different letters indicate statistical significant differences among groups (p<0.05).
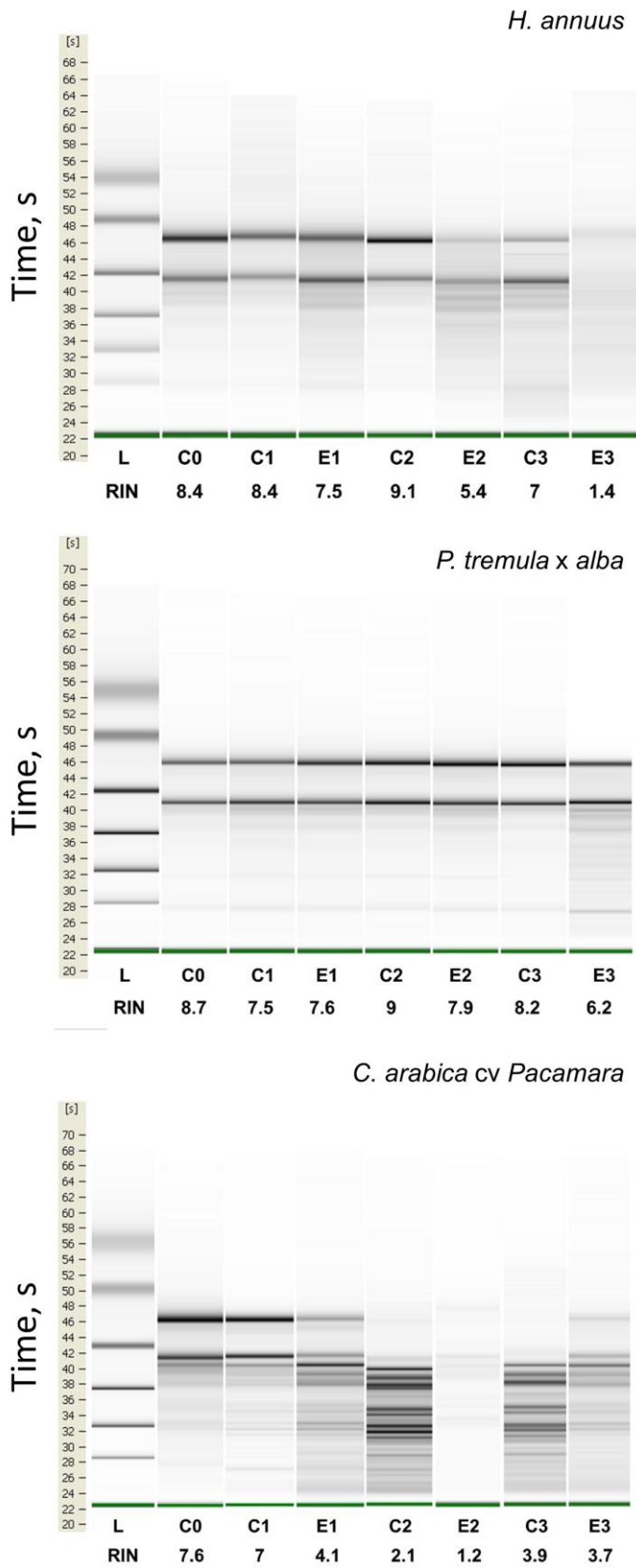
Fig. 4: Evaluation of RNA integrity by Bioanalyzer assay. For each RNA sample, extracted from control (C) or exposed plant stems (E), the related RIN (RNA integrity number) is provided below each lane of the gel. L = ladder.